

PROFILE CONTROL WITH LOWER HYBRID WAVES ON ASDEX

F.X. Söldner, K. McCormick, F. Leuterer, and G. Becker, H.S. Bosch, H. Brocken, A. Carlson, A. Eberhagen, G. Dodel¹, H.-U. Fahrbach, G. Fussmann, O. Gehre, J. Gernhardt, G. v.Gierke, E. Glock, O. Gruber, G. Haas, W. Herrmann, J. Hofmann, A. Izvozhikov², E. Holzhauser¹, K. Hübner³, G. Janeschitz, F. Karger, M. Kaufmann, O. Klüber, M. Kornherr, K. Lackner, M. Lenoci, G. Lisitano, F. Mast, H.M. Mayer, D. Meisel, V. Mertens, E.R. Müller, M. Münich, H. Murmann, J. Neuhauser, H. Niedermeyer, A. Pietrzyk⁴, W. Poschenrieder, H. Rapp, H. Riedler, A. Rudyj, F. Schneider, C. Setzensack, G. Siller, E. Speth, K. Steinmetz, K.-H. Steuer, N. Tsois⁵, S. Ugniewski⁶, O. Vollmer, F. Wagner, D. Zasche, M. Zouhar

Max-Planck-Institut für Plasmaphysik,
EURATOM Association, Garching, FRG

Introduction

Optimization of plasma current profiles may be a way to provide stability against MHD modes /1/. With inductive current drive, however, external control is impeded by the link between current density and electron temperature profiles. RF current drive therefore has been proposed for local profile shaping /2/. The largest current drive efficiency in a wide range of experimental applications has been obtained with Lower Hybrid current drive. Modification of the current profile and decoupling of $j(r)$ and $T_e(r)$ were demonstrated on ASDEX /3, 4/. In this paper the correlation between current profile changes and the behavior of MHD modes is studied. Local profile shaping by tailoring of the launched LH wave spectrum is investigated. The impact on electron density and temperature profiles and the relevance of profile consistency are discussed.

The form of the current density profile $j(r)$ can be characterized by the internal inductance l_i . From the two independent measurements of $\beta_p^{qu} + l_i/2$ and of the diamagnetic β_p^d , the sum of l_i and of the anisotropy in electron pressure, $l_i + (\beta_p^a - \beta_p^d)$ may be determined. With LH current drive both quantities may vary in time but the different time scales allow separation of the two parts in most cases. Direct measurements of the current distribution $j(r)$ were made for typical cases also with a Li-beam diagnostic /5/. The change in the internal inductance Δl_i as determined by both diagnostics is plotted in fig. 1 versus rf-power for LH-current drive in the density range $\bar{n}_e = 0.5 - 1.6 \times 10^{13} \text{ cm}^{-3}$. An increase of l_i and therefore peaking of $j(r)$ is obtained at low rf-power. The suprathermal electrons generated by the LH are accelerated in this case to very high energies by the initial high dc electric field as indicated by a continuous increase of hard X-ray radiation /6/. With higher LH-powers the loop voltage is reduced and a suprathermal electron distribution with an upper boundary of $\sim 400 \text{ keV}$ is maintained. The current distribution $j(r)$ broadens under these con-

¹ University of Stuttgart; ² Ioffe Institute; ³ University of Heidelberg;

⁴ University of Washington, Seattle, USA; ⁵ N.R.C.N.S. "Democritos",

Athens, Greece; ⁶ Inst. for Nuclear Research, Swierk, Poland;

ditions and l_i decreases as P_{LH} increases. The current distribution therefore is closely related to the form of the electron distribution function which is determined by the combination of inductive and rf-current drive. At high LH-power strong central electron heating results in a peaking of $T_e(r)$ while $j(r)$ is flattened. Thus, the resistive link between current and temperature profiles is then removed with LH-current drive.

Sawtooth oscillations are strongly influenced by modifications of the current profile. Peaking of $j(r)$ at low P_{LH} leads to an augmentation of the sawtooth amplitude. Above a threshold LH-power sawteeth are completely suppressed when $j(r)$ is flattened such that $q > 1$ in the whole plasma /7/. Sawteeth can also be stabilized by this method in the presence of strong additional heating from NBI /8/. In the sawtooth-free phase higher central electron temperatures are obtained. The electron density also peaks with the steady-state profile being similar to that just before the sawtooth crash.

Steady-state sawtooth-free discharges can be maintained for the whole duration of the rf pulse (≤ 1.5 s) with LH powers slightly above the threshold for sawtooth stabilization (30-50 % of the power required for complete current drive). If the LH power is further increased MHD modes with mode numbers $m=2,3$ / $n=1$ may be activated. The various regimes are shown in fig. 2 for a density scan with LH-current drive at constant power $P_{LH}=750$ kW. Δl_i is plotted together with a signal from Li-beam measurements $\Delta\theta_p(r=15$ cm) which is proportional to the change in fractional plasma current inside $r=15$ cm. At low density strong broadening of $j(r)$ with a resulting reduction of the internal inductance $-\Delta l_i$ up to 0.3 leads to the onset of $m=2$ modes several hundred ms after the stabilization of sawteeth. The total plasma current is driven by the LH in this density range. With increasing density the drop in l_i decreases. Sawteeth are still stabilized up to $\bar{n}_e=1.6 \times 10^{13}$ cm $^{-3}$ where $-\Delta l_i=0.15$. Steady state discharges stable against sawteeth and other MHD modes are thus obtained in the density range $\bar{n}_e=0.8-1.6 \times 10^{13}$ cm $^{-3}$. Towards higher densities the signal $\Delta\theta_p(r=15$ cm) decreases faster than $-\Delta l_i$. Above $\bar{n}_e=2 \times 10^{13}$ cm $^{-3}$ the current distribution is no longer modified in the central region while the total current profile still broadens. This may be explained by a local flattening of $j(r)$ by the LH which is shifted towards the periphery with increasing density. With edge current drive a redistribution of the current in the center is not seen during pulse times of 1s possibly due to the long inductive time constants.

$m=2$ modes are readily destabilized by LH-current drive at low $q(a)$. They appear shortly after suppression of sawteeth. In experiments at $q(a)=2.1$, $m=2$ modes are triggered immediately after begin of the rf pulse. In most cases they give rise to major disruptions. Sawteeth could not be stabilized under these conditions. With decreasing $q(a)$ rf-generated modifications of the Ohmic $j(r)$ profile therefore increasingly provoke mode activity for the LH spectra investigated here. This may be caused by a steepening of $V_p j(r)$ in the region of the $q=2$ surface due to the current redistribution.

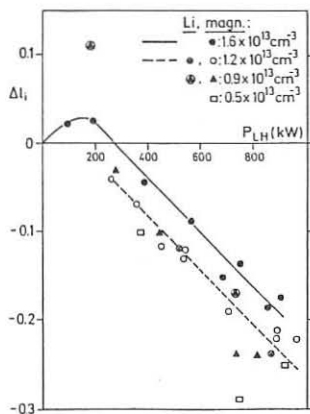


Fig. 1: Variation of ΔI_i with P_{LH} during LH-current drive, from magnetic and Li-beam measurements.

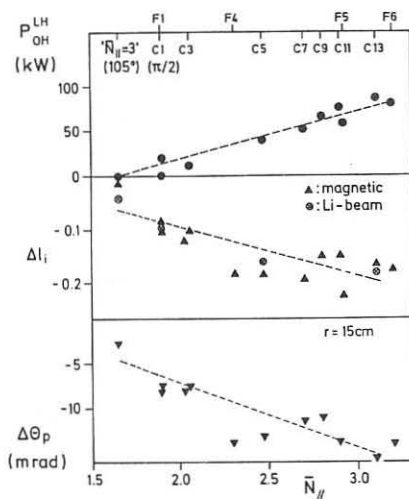


Fig. 3: Residual Ohmic power input P_{OH} , ΔI_i and $\Delta\theta_p(r=15\text{ cm})$ for LH-current drive with $P_{LH}=350\text{ kW}$ at different \bar{N}_{\parallel} . $I_p=300\text{ kA}$, $B_t=2.17\text{ T}$.

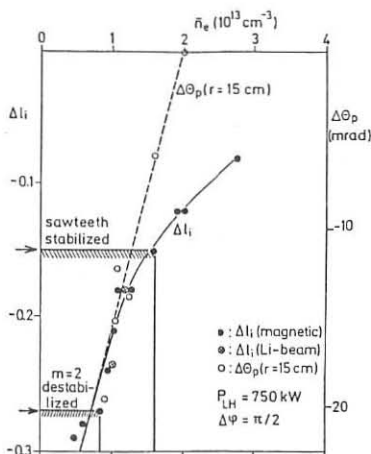


Fig. 2: Variation of ΔI_i and of the monitor signal $\Delta\theta_p(r=15\text{ cm})$ with \bar{n}_e . $I_p=300\text{ kA}$, $B_t=2.17\text{ T}$, $q(a)=3.5$.

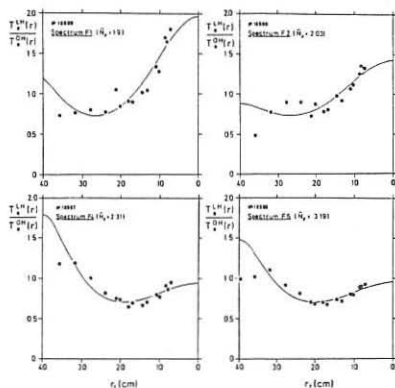


Fig. 4: Change of the electron temperature profile for different LH-current drive spectra.

Optimization of the current profile with respect to all modes therefore requires selective modification of $j(r)$ with external control of the local absorption of the LH waves. In a series of experiments the shape of the LH wave spectrum was varied by adjusting the power fed into each one of the waveguides of the grill antenna /9/. Thereby \bar{N} could be varied in the range $1.9 < \bar{N} < 3.2$ with highly directional current-drive spectra. The plasma current was kept constant at 300 kA by feedback control. The variation during LH of the residual Ohmic power input P_{OH}^{LH} , of ΔI_1 and $\Delta \theta_p$ ($r=15$ cm) are shown in fig. 3. The results with a wider grill ($N(\Delta\phi=\pi)=3$) at $\Delta\phi=105^\circ$, $\bar{N}=1.65$ are also included in this figure. With increasing \bar{N} the current-drive efficiency is reduced as expected from theory. Therefore the additional Ohmic input P_{OH}^{LH} has to be increased. The change of the current profile characterized by ΔI_1 and $\Delta \theta_p$ ($r=15$ cm), however, is enhanced with increasing \bar{N} , i.e. with decreasing rf-driven current. This can be explained only by a shift of the LH current deposition zone to larger radii and a resulting flattening of $j(r)$ closer to the plasma surface. This is confirmed by local current profile measurements. They show also an increase of $-\Delta I_1$ with \bar{N} but simultaneously a decrease of the change of $j(r)$ in the center:

$$\begin{aligned} \bar{N}=1.65: & -\Delta I_1=0.04, \Delta q(0)=0.3 \\ \bar{N}=3.1: & -\Delta I_1=0.16, \Delta q(0)=0.11. \end{aligned}$$

The displacement of the LH deposition zone is also clearly seen in the modification of the electron temperature profiles as shown in fig. 4. The ratio $T_e^{LH}(r)/T_e^0(r)$ of the local values is calculated at each radius; the points in fig. 4 refer to the actual data points, the solid lines to fitted analytic profiles for $T_e(r)$. This form of local normalization of the profiles leads to a better criterion for profile consistency which then would require a constant factor of temperature change for all radii, i.e. straight horizontal lines in fig. 4. With LH-current drive, strong electron heating is achieved in the center for low \bar{N} , while edge heating and cooling of the center are observed at high \bar{N} . This shows that a large variety of electron temperature profiles can be obtained with LH current drive which are not subject to profile consistency.

As shown in these experiments, the form of current and temperature profiles is governed by the local deposition of LH power. The position of the absorption zone can be varied externally by varying the launched wave spectrum. This allows for an active control of plasma profiles, where sawteeth and MHD modes with higher m numbers might be suppressed simultaneously.

References

- /1/ A.H. Glasser, et al., Phys. Rev. Lett. 38, 234 (1977)
- /2/ A.H. Reiman, Phys. Fluids 26, 1338 (1983)
- /3/ K. McCormick, et al., 12th Europ. Conf. on Contr. Fusion and Plasma Physics, Budapest 1985, Vol. I, p. 199
- /4/ K. McCormick, et al., Phys. Rev. Lett. 58, 491 (1987)
- /5/ K. McCormick, et al., 13th Europ. Conf. on Contr. Fusion and Plasma Physics, Schliersee, 1986, Vol. Vol. II, p. 323
- /6/ F.X. Söldner, et al., internal report IPP II/111 (1986)
- /7/ F.X. Söldner, et al., Phys. Rev. Lett. 57, 1137 (1986)
- /8/ F.X. Söldner, et al., ref. 5, Vol. II, p. 319
- /9/ F. Leuterer, et al., ref. 5, Vol. II, p. 409